

Universal Symmetry Constraints on Spin Polarization in Non-centrosymmetric Crystals

Wei Tan,^{1,*} Jianfeng Wang,^{2,*} Yang Li,¹ and Bing Huang^{1,3,†}

¹Beijing Computational Science Research Center, Beijing 100193, China

²School of Physics, Beihang University, Beijing 100191, China

³Beijing Normal University, Beijing 100875, China

(Dated: December 6, 2023)

The current understanding of spin-polarization phenomena in crystals relying on the crystalline symmetries is far from complete. Here, we develop a universal theory, consisting of five basic rules, to capture the diverse spin textures (STs) in non-centrosymmetric crystals, exhaustively classifying the non-centrosymmetric symmetry operations and in particular their combination with time-reversal symmetry in symmetry-protected k -invariant subspace. Our theory is verified by extensive material examples based on the first-principles calculations, explaining their kaleidoscopic STs or even vanishing spin-polarization effect. Interestingly, based on our theory, we argue that the generally accepted radial STs in chiral crystals cannot be rigorous. More importantly, combining with topological band theory, we propose the three-dimensional symmetry-enforced persistent STs, which is long sought but never be discovered, could be abundant in two families of nonsymmorphic crystals. Our theory could broaden our understanding of spin-polarization effect and enable the dream of *ab initio* design of desirable STs in crystals.

Introduction. Symmetry is the basis of the universe. In condensed matter, crystalline symmetry provides a fundamental framework to understand or predict a wide range of physical phenomena. For examples, in crystals with PT symmetry, the presence of spin-orbital coupling (SOC) effect can induce the degeneracy of energy bands, generating hidden spin polarization [1–4]. When PT symmetry is broken, SOC effect can lift the degeneracy of energy bands, leading to nonzero spin polarization [5]. Importantly, many interesting spin-related phenomena, such as Edelstein effect [6–10], spin-orbit torque [11–14], spin galvanic effects [15–17] and spin relaxation [18–23], attribute to their unique spin textures (STs), which consist of the spin-polarization vectors of different k points in Brillouin zone (BZ). The ST reveals the inherent interplay between charge and spin degrees under both crystal field and external field.

In history, the most famous STs are Rashba and Dresselhaus ones, which were initially discovered in wurtzite [5, 24, 25] and zinc-blende [5, 26] crystals more than half a century ago. Recently, the emergence of unexpectedly new STs, *e.g.*, radial STs in chiral crystal (such as elemental Te [27–29]) and two-dimensional (2D) persistent STs (PSTs) in non-centrosymmetric systems with point groups of C_{3h} and D_{3h} (such as $\text{Ge}_3\text{Pb}_5\text{O}_{11}$ [30]), stimulates intensive interests to explore their physical origin [31–35]. While the traditional way to understand these STs heavily relies on the establishment of point-group-dependent low-order effective Hamiltonians [5, 24–27, 30, 33–35], a universal theory that solely depends on the symmetry argument to capture the origin of STs is still lacking, preventing the design of desirable STs for spintronics, *e.g.*, the real 3D PSTs with long spin decoherence time.

In this Letter, we have developed a universal theory, consisting of five independent symmetry-constrained rules, to understand the dramatically changeable STs in non-centrosymmetric crystals. Importantly, we enumerate all the non-centrosymmetric crystalline-symmetry operations and

their combinations with time-reversal operation (T) for arriving these rules. Our theory is verified by material examples using first-principles density-functional theory (DFT) calculations (see **Method** [36]), explaining their variable STs or even the appearance of zero spin-polarization lines (ZSPLs). Based on our theory, we demonstrate that the widely believed radial STs in chiral crystals cannot be rigorous. Finally, combining with topological band theory, we propose the symmetry-constrained 3D PSTs could be very abundant in two big families of nonsymmorphic crystals.

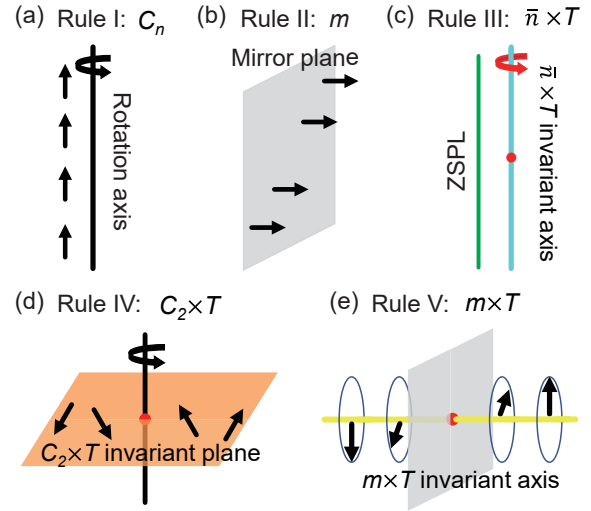


FIG. 1. Complete rules of spin-polarization. (a) *Rule I*: along rotation axis (C_2 , C_3 , C_4 and C_6), only parallel spin-polarization component can exist. (b) *Rule II*: in mirror plane, only perpendicular spin-polarization component can exist. (c) *Rule III*: along $\bar{n} \times T$ -invariant axis (\bar{n} represents roto-inversion $\bar{4}$ and $\bar{6}$), a ZSPL is obtained (denoted by green-line). (d) *Rule IV*: in $C_2 \times T$ -invariant plane, only in-plane spin-polarization component can exist. (e) *Rule V*: along $m \times T$ -invariant axis, only perpendicular spin-polarization component can exist. Arrows indicate the directions of spin-polarization vectors. Red-dots represents time-reversal-invariant-momenta (TRIMs).

Complete Rules for Spin-polarization. Considering a general crystalline-symmetry operation (e.g., mirror m or two-fold rotation C_2) or its combination with T (e.g., $m \times T$ or $C_2 \times T$), it will keep some wave-vectors k invariant in BZ. These invariant k constitute a subspace $M[O]$ [37]. And the observable spin-polarization vector component $\langle S_i^{(n,k)} \rangle = \langle \psi(n, k) | \hat{S}_i | \psi(n, k) \rangle$ is severely constrained by the symmetry O on $M[O]$ ($i = x, y, z$; n =band index). For example, PT symmetry flips spin-polarization vector \vec{S} but preserves k in the whole BZ, thus generating spin degeneracy or even hidden spin polarization in some nonmagnetic centrosymmetric crystals [1] and anti-ferromagnetic crystals [3].

Here, we explore the symmetry constraints on $\langle S_i^{(n,k)} \rangle$ in non-centrosymmetric systems. For each space group, its crystalline-symmetry operations can be represented by its generators. By enumerating all these generators for non-centrosymmetric space groups (Table S1 [36]), we could classify them into three classes: rotation/screw-rotation, mirror/glide-mirror, and roto-inversion operations (Table S2 [36]). Combining with T and temporarily ignoring fractional translations in consideration of ST in k space, we obtain five basic rules of symmetry constraint on spin-polarization:

(i) C_n -constrained Parallel Spin-polarization: Without loss of generality, considering a n -fold rotation symmetry along z direction (C_{nz}), C_{nz} acts in both momentum space (k_x, k_y, k_z) and spin space (S_x, S_y, S_z) simultaneously,

$$\begin{aligned} C_{nz} : (k_x, k_y, k_z) &\rightarrow (C_{nz}k_x, C_{nz}k_y, k_z) \\ (S_x, S_y, S_z) &\rightarrow (C_{nz}S_x, C_{nz}S_y, S_z). \end{aligned} \quad (1)$$

Thus, in C_{nz} -preserved $M[C_{nz}]$, one has $(\langle S_x^{(n,k)} \rangle, \langle S_y^{(n,k)} \rangle, \langle S_z^{(n,k)} \rangle) = (C_{nz}\langle S_x^{(n,k)} \rangle, C_{nz}\langle S_y^{(n,k)} \rangle, \langle S_z^{(n,k)} \rangle)$, and deduce that $\langle S_x^{(n,k)} \rangle$ and $\langle S_y^{(n,k)} \rangle$ are exactly zero. Therefore, only parallel $\langle S_z^{(n,k)} \rangle$ are nonzero in $M[C_{nz}]$ [Fig. 1(a), Rule I].

(ii) m -constrained Perpendicular Spin-polarization: Considering a generic mirror symmetry perpendicular to y axis (m_y), we have

$$\begin{aligned} m_y : (k_x, k_y, k_z) &\rightarrow (k_x, -k_y, k_z) \\ (S_x, S_y, S_z) &\rightarrow (-S_x, S_y, -S_z). \end{aligned} \quad (2)$$

Thus, in m_y -preserved $M[m_y]$, one has $(\langle S_x^{(n,k)} \rangle, \langle S_y^{(n,k)} \rangle, \langle S_z^{(n,k)} \rangle) = (-\langle S_x^{(n,k)} \rangle, \langle S_y^{(n,k)} \rangle, -\langle S_z^{(n,k)} \rangle)$, and deduce that $\langle S_x^{(n,k)} \rangle$ and $\langle S_z^{(n,k)} \rangle$ are exactly zero. Therefore, only out-of-plane $\langle S_y^{(n,k)} \rangle$ is allowed in $M[m_y]$ [Fig. 1(b), Rule II].

(iii) $\bar{n} \times T$ -constrained ZSPL: Considering a generic fourfold roto-inversion symmetry along z direction with T ($\bar{4}_z \times T$), we have

$$\begin{aligned} \bar{4}_z \times T : (k_x, k_y, k_z) &\rightarrow (-k_y, k_x, k_z) \\ (S_x, S_y, S_z) &\rightarrow (S_y, -S_x, -S_z). \end{aligned} \quad (3)$$

Thus, in $\bar{4}_z \times T$ -preserved $M[\bar{4}_z \times T]$, one has $(\langle S_x^{(n,k)} \rangle, \langle S_y^{(n,k)} \rangle, \langle S_z^{(n,k)} \rangle) = (\langle S_y^{(n,k)} \rangle, -\langle S_x^{(n,k)} \rangle, -\langle S_z^{(n,k)} \rangle)$, and deduce that all $\langle S_i^{(n,k)} \rangle$ are exactly zero, forming a ZSPL along

$\bar{4}_z \times T$ -invariant axis. A similar conclusion holds for $\bar{6}_z \times T$ [Fig. 1(c), Rule III].

(iv) $C_2 \times T$ -constrained In-plane Spin-polarization: Considering a generic C_{2z} with T ($C_{2z} \times T$), we have

$$\begin{aligned} C_{2z} \times T : (k_x, k_y, k_z) &\rightarrow (k_x, k_y, -k_z) \\ (S_x, S_y, S_z) &\rightarrow (S_x, S_y, -S_z). \end{aligned} \quad (4)$$

Thus, in $C_{2z} \times T$ -preserved $M[C_{2z} \times T]$, one has $(\langle S_x^{(n,k)} \rangle, \langle S_y^{(n,k)} \rangle, \langle S_z^{(n,k)} \rangle) = (\langle S_x^{(n,k)} \rangle, \langle S_y^{(n,k)} \rangle, -\langle S_z^{(n,k)} \rangle)$, and deduce that $\langle S_z^{(n,k)} \rangle$ is exactly zero. Therefore, only in-plane $\langle S_x^{(n,k)} \rangle$ and $\langle S_y^{(n,k)} \rangle$ are nonzero in $M[C_{2z} \times T]$ [Fig. 1(d), Rule IV].

(v) $m \times T$ -constrained Perpendicular Spin-polarization: Considering a generic m_y with T ($m_y \times T$), we have,

$$\begin{aligned} m_y \times T : (k_x, k_y, k_z) &\rightarrow (-k_x, k_y, -k_z) \\ (S_x, S_y, S_z) &\rightarrow (S_x, -S_y, S_z). \end{aligned} \quad (5)$$

Thus, in $m_y \times T$ -preserved $M[m_y \times T]$, one has $(\langle S_x^{(n,k)} \rangle, \langle S_y^{(n,k)} \rangle, \langle S_z^{(n,k)} \rangle) = (\langle S_x^{(n,k)} \rangle, -\langle S_y^{(n,k)} \rangle, \langle S_z^{(n,k)} \rangle)$, and deduce that $\langle S_y^{(n,k)} \rangle$ is exactly zero. Therefore, parallel $\langle S_x^{(n,k)} \rangle$ are forbidden in $M[m_y \times T]$ [Fig. 1(e), Rule V].

While Rules I and II may be partially indicated in the literature [31, 38], to best of our knowledge, Rule III-V are proposed for the first time forming a complete theory. In addition, the above conclusion can also apply to nonsymorphic symmetries including the fractional translations. In terms of Rule I-V, we can realize that the \vec{S} is always parallel to rotation axis and $C_2 \times T$ -invariant plane, perpendicular to mirror plane and $m \times T$ -invariant axis, or exhibits a ZSPL along $\bar{n} \times T$ -invariant axis, at the symmetry-preserved k -invariant regions. In principle, these individual rules or their combinations can be applied to understand the framework of kaleidoscopic STs in non-centrosymmetric crystals, even without the knowledge of their specific Hamiltonians.

Based on the rules, it is interesting to further understand the emergence of ZSPLs, which can be classified into two types. Type-I is pinned ZSPL, (including two major cases: (i) According to Rule III, there is a pinned ZSPL along $\bar{n} \times T$ -invariant axis; (ii) Combining Rules I and II, when two mirror symmetries are included and related by rotation (e.g., m_x and m_y , and $C_{2z} = m_x \times m_y$), a ZSPL is formed and pinned along the intersecting lines of m_x and m_y , i.e., the C_{2z} axis [39]. Type-II is unpinned ZSPL: Combining Rule II with T (e.g., a TRIM point is located in the mirror plane), only perpendicular $\langle S_i^{(n,k)} \rangle$ is allowed in mirror plane, while the presence of T flips $\langle S_i^{(n,k)} \rangle$ from $+k$ point to $-k$ point, i.e., $\langle S_i^{(n,k)} \rangle = -\langle S_i^{(n,-k)} \rangle$, thus creating at least one unpinned boundary line with zero spin-polarization, which separates the regions with opposite perpendicular spin-polarizations. Therefore, at least one unpinned ZSPL exists in such single mirror plane of nonmagnetic non-centrosymmetric crystals.

Material Verification. The crystals with low point-group symmetries, e.g., C_2 , C_3 and S_4 , are selected to confirm our rules. The first example is I_4Ti_2Zn . As shown in Fig. 2(a), black-line and orange-plane represent rotation axis and $C_2 \times$

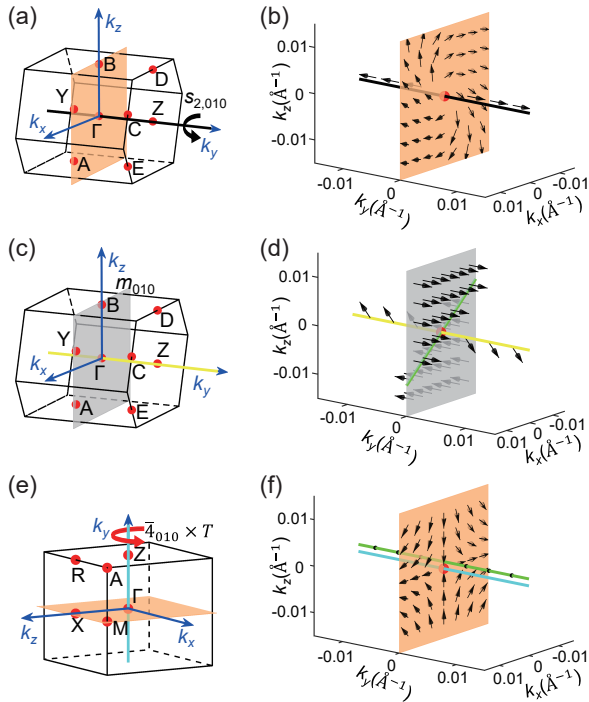


FIG. 2. **DFT-calculated spin textures centered at Γ -point.** (a) First BZ and (b) STs of I_4Tl_2Zn (space group $P2_1$). (c) First BZ and (d) STs of ReN_2 (space group Pm). (e) First BZ and (f) STs of $GeSe_2$ (space group $P4$). Red-dots represents TRIMs. Green-line represents ZSPL. Here, STs are plotted for the band near Fermi-level. We note that the features of STs are determined by our rules and independent of the selected bands (Figs. S1-S3 [36]).

T -invariant plane in BZ, respectively. I_4Tl_2Zn has a twofold screw-rotation $s_{2,010} = \{C_{2,010} | 0 \ 1/2 \ 0\}$ along y direction. In Fig. 2(b), DFT-calculations show that: (i) Only parallel $\langle S_y^{(n,k)} \rangle$ is allowed along k_y axis (rotation axis), confirming **Rule I**. (ii) Only in-plane $\langle S_x^{(n,k)} \rangle$ and $\langle S_z^{(n,k)} \rangle$ are nonzero in $k_y=0$ ($C_2 \times T$ -invariant plane), confirming **Rule IV**.

The second example is ReN_2 . As shown in Fig. 2(c), yellow-line and grey-plane represent $m \times T$ -invariant axis and mirror plane, respectively. There is only a single mirror symmetry m_{010} perpendicular to y axis. In Fig. 2(d), DFT-calculations reveal that: (i) Parallel $\langle S_y^{(n,k)} \rangle$ is forbidden along k_y axis ($m \times T$ -invariant axis), confirming **Rule V**. (ii) Only perpendicular $\langle S_y^{(n,k)} \rangle$ is nonzero in $k_y=0$ plane (mirror plane), confirming **Rule II** and meanwhile forming 2D PSTs. Thus, we can image that abundant non-centrosymmetric materials with mirror symmetry can possess 2D PSTs, providing a more fundamental explanation for the observed 2D PSTs in many reported materials [30, 38, 40]. Interestingly, there exists one type-II ZSPL in the single mirror plane [green-line in Fig. 2(d)], separating the regions with opposite perpendicular \vec{S} . The position of ZSPL is changeable for different energy bands (Fig. S2 [36]).

The third example is $GeSe_2$. As shown in Fig. 2(e), cyan-line and orange-plane represent $\bar{n} \times T$ -invariant axis and $C_2 \times T$ -

invariant plane, respectively. There is a roto-inversion $\bar{4}_{010}$ and a twofold-rotation $C_{2,010}$ along y axis. Using DFT calculations, we find that: (i) Type-I ZSPL appears along k_y axis ($\bar{4}_{010} \times T$ -invariant axis), confirming **Rule III**. Differing from Fig. 2(d), the position of ZSPL is fixed for different bands (Fig. S3 [36]). (ii) Only in-plane $\langle S_x^{(n,k)} \rangle$ and $\langle S_z^{(n,k)} \rangle$ are nonzero in $k_y=0$ plane ($C_2 \times T$ -invariant plane) [Fig. 2(f)], confirming **Rule IV**. Besides these three typical examples, we have done extensively material examples to confirm the universality of our rules (Figs. S4-S17 [36]).

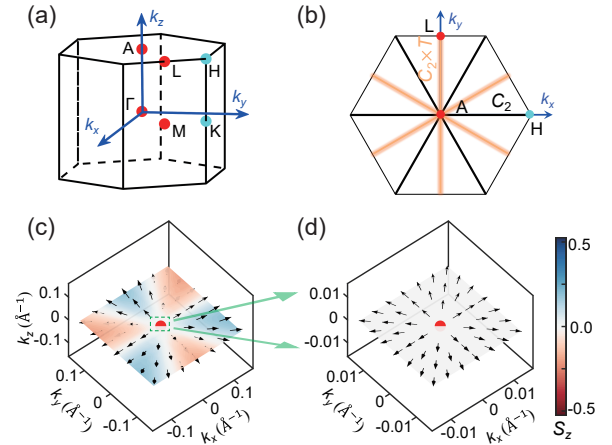


FIG. 3. **Spin textures in chiral Tellurium.** (a) Side and (b) top views of first BZ for Tellurium. In (b), black- and orange-lines represent twofold-rotation axes and $C_2 \times T$ -invariant planes, respectively. DFT-calculated spin textures in $k_z=\pi$ plane centered at A point within (c) $|k| \sim 0.1 \text{ \AA}^{-1}$ and (d) $|k| \sim 0.01 \text{ \AA}^{-1}$, respectively. Calculated band is the second lowest conduction band. Colors in plane represent the magnitude of out-of-plane $\langle S_z^{(n,k)} \rangle$. Red- and cyan-dots represent TRIMs and non-TRIMs, respectively.

Spin Texture of Chiral Crystal. Our rules can present a deeper understanding of some unusual STs in crystals, *e.g.*, the proposed radial STs in chiral crystals [27–29]. Taking quasi-1D Tellurium (Te) with space group $P3_221$ as an example, its first BZ is plotted in Fig. 3(a). As shown in Fig. 3(b), there is one threefold screw-rotation along z axis, three twofold C_2 rotations along A-H paths and three $C_2 \times T$ -invariant planes [orange-lines from top view in Fig. 3(b)] perpendicular to A-H paths. According to Rule I, the \vec{S} are exactly parallel along A-H paths, which provides a rigorously radial backbone [41]. According to Rule IV, the \vec{S} are exactly constrained in $C_2 \times T$ -invariant planes but with undetermined directions, that is, there is no guarantee for the \vec{S} being radial along A-L paths where only three $C_2 \times T$ -invariant planes exist.

To confirm our speculation, DFT-calculated STs in $k_z=\pi$ plane are shown in Fig. 3(c). Indeed, radial \vec{S} only exist along three A-H paths, and there are obviously nonzero $\langle S_z^{(n,k)} \rangle$ components in other k points including three A-L paths. Therefore, the purely radial STs could not exist in Te, contrary to the generally accepted conclusion [27–29, 31]. Only if the BZ is constrained to a sufficiently small region [Fig. 3(d)], the

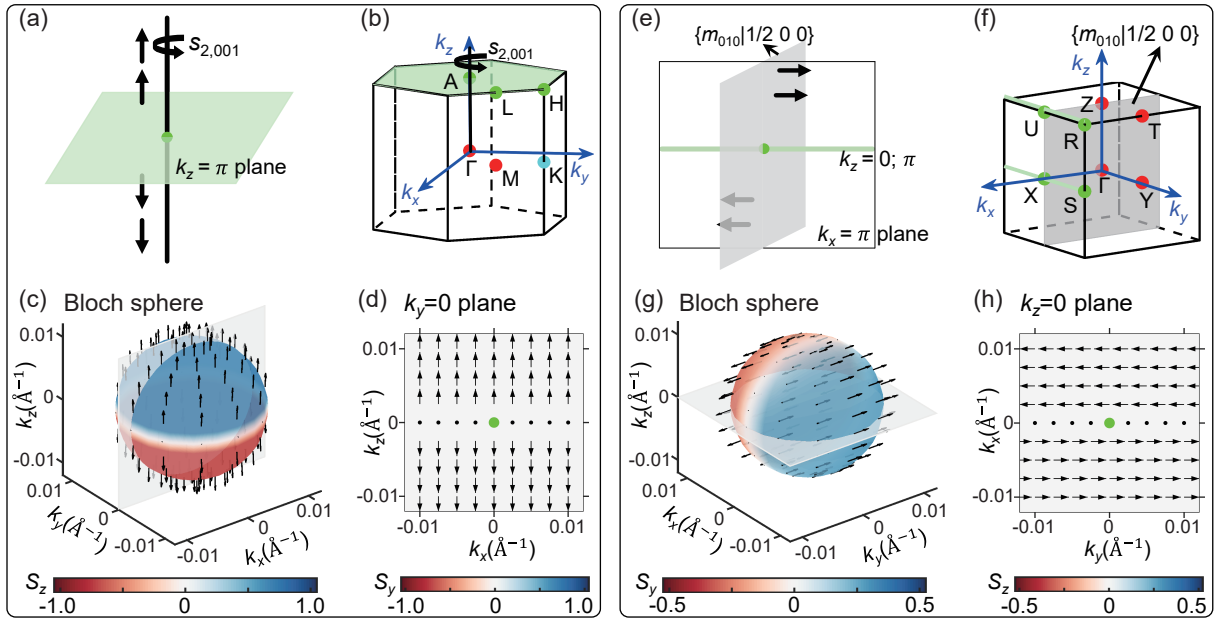


FIG. 4. **3D persistent spin texture.** (a) Principle of 3D PST produced by two-fold screw-rotation in combination with T . (b) First BZ of material example PI_3 (space group $P6_3$). A twofold screw-rotation $s_{2,001} = \{C_{2,001} | 0 0 1/2\}$ is along z axis. Green-plane represents a nodal-plane. Green-dots represent high-symmetry points generating 3D PSTs. (c) DFT-calculated 3D PST surrounding A point, where spin-polarization is along z direction. (d) PST from an arbitrary 2D cut-plane marked in (c). (e) Principle of 3D PST produced by glide-mirror in combination with T . (f) First BZ of material example PbS (space group $Pma2$). A glide mirror $\tilde{m}_{010} = \{m_{010} | 1/2 0 0\}$ perpendicular to y axis exists. Green-lines represent the nodal-lines. (g) DFT-calculated 3D PST surrounding R point, where spin-polarization is along y direction. (h) PST from an arbitrary 2D cut-plane marked in (g).

radial-like STs may exist with sufficiently small spin components of $\langle S_z^{(n,k)} \rangle$. In fact, the emergence of radial ST in Te is the result of combined action of multiple rotation symmetries under k -linear approximation of $k \cdot p$ Hamiltonians, in which the threefold screw-rotation operation is equivalent to an n -fold rotation operation ($n \rightarrow \infty$). Indeed, whether purely radial STs can exist in chiral systems is also questioned based on the complicated high-order terms in Hamiltonians [35].

Symmetry-constrained 3D PSTs. While **Rule II** indicates 2D PSTs can appear in mirror plane of crystals, whether a full-space 3D PST can exist is still a mystery, as it is never discovered in a real system. Here, combining our rules with topological band theory, importantly, we propose that two cases of symmetry-constrained 3D PSTs can exist. Case-I is generated by two-fold screw-rotation having a parallel fractional translation in combination with T (left-panel, Fig. 4). As shown in Fig. 4(a), according to **Rule I**, only parallel $\langle S_z^{(n,k)} \rangle$ is nonzero along k_z rotation axis. For a nonmagnetic crystal with a generic twofold screw-rotation $s_{2,001}$, the \vec{S} is (almost) null in $k_z = \pi$ plane, where a $s_{2,001} \times T$ enforced nodal plane is formed based on topological band theory [42–45], thus generating spin degeneracy. Especially, when the only retained k -linear term $k_z \sigma_z$ is dominated in $k \cdot p$ Hamiltonian, the \vec{S} surrounding the high-symmetry point of BZ boundary is uniformly aligned along screw-rotation axis, forming a 3D PST. To confirm our idea, we select PI_3 material (space group $P6_3$) as an example, whose first BZ is shown in Fig. 4(b). There is

a twofold screw-rotation $s_{2,001}$ along z axis and a $s_{2,001} \times T$ -enforced nodal-plane at $k_z = \pi$ plane. The calculated 3D STs of second-lowest conduction band surrounding A point are shown in Fig. 4(c), which exhibit two features: i) 3D PSTs along z direction exist in the full Bloch sphere where k -linear term $k_z \sigma_z$ is dominated; Fig. 4(d) further shows the slice of 3D PST in 2D cut-plane. ii) The direction of \vec{S} flips from $+z$ in $k_z > 0$ to $-z$ in $k_z < 0$, due to T symmetry. Interestingly, the existence of 3D PSTs is independent of the specific energy band and can be described by $k_z \sigma_z$ (Figs. S19-S20 [36]), which are also found around L and H points (Fig. S18 [36]). 3D PST can be maintained within a large radius of 0.1 \AA^{-1} (Fig. S21 [36]). Besides of PI_3 , Case-I 3D PSTs are also observed in Ag_2Se (space group $P2_12_12_1$) due to the similar reason (Fig. S26 [36]).

Case-II 3D PST is generated by glide-mirror having at least a parallel fractional translation in combination with T (right panel, Fig. 4). As shown in Fig. 4(e), according to **Rule II**, only perpendicular $\langle S_y^{(n,k)} \rangle$ are nonzero in mirror plane. For the nonmagnetic systems with a generic glide-mirror $\tilde{m}_{010} = \{m_{010} | 1/2 0 0\}$, \vec{S} is almost null along y direction in $k_x = \pi$ plane, where $\tilde{m}_{010} \times T$ -enforced nodal lines are formed based on topological band theory [43–46]) and the fractional translation determines the positions of nodal lines. Similarly, when the only retained k -linear term $k_x \sigma_y$ is dominated in $k \cdot p$ Hamiltonian, \vec{S} surrounding the high-symmetry point of BZ boundary is uniformly aligned perpendicular to

the glide-mirror plane. Again, to confirm our design principle, we select PbS material (space group $Pma2$) as an example, whose first BZ is shown in Fig. 4(f). There is a glide-mirror \tilde{m}_{010} perpendicular to y axis and two nodal-lines along U-R and X-S in the BZ. The calculated 3D STs of lowest conduction band surrounding R point are shown in Fig. 4(g), which also exhibit two features: i) 3D PSTs along y direction exist in the full Bloch sphere where k -linear term $k_x\sigma_y$ is dominated; Fig. 4(h) further shows the slice of 3D PST in 2D cut-plane. ii) The direction of \vec{S} flips from $+y$ in $k_x < 0$ to $-y$ in $k_x > 0$. The existence of 3D PSTs is independent of the specific energy band and can be described by $k_x\sigma_y$ (Figs. S23-S24 [36]), which are also found around X, S and U points (Fig. S22 [36]) and almost maintained within a large radius of 0.1 \AA^{-1} (Fig. S25 [36]). Besides of PbS, Case-II 3D PSTs are also observed in $\text{Ba}_2\text{Ti}(\text{GeO}_4)_2$ (space group $P4bm$) (Fig. S27 [36]). It is noted that in a system with more than one nonsymmorphic symmetry, the additional presence of s_2 or \tilde{m} will affect the band-crossing at the specific boundary-points of BZ [47], in which 3D PSTs could be broken (Figs. S26-S27 [36]).

Outlook. We emphasize that the interesting concept of chirality-induced spin selectivity (CISS) [48, 49] in chemistry can also be understood based on our theory. For example, since DNA-like molecule holds twofold screw-rotation symmetry, similar to Case-I 3D PSTs, a symmetry-constrained PST will appear, which could create significant circular dichroism.

We have revealed the general theory of spin polarization in non-centrosymmetric crystals. For a system with a given symmetry (regardless nonmagnetic or magnetic), our theory can provide a framework for its ST in entire BZ. At a generic k point out of symmetry-preserved k -invariant subspace, its detailed ST may vary in different materials even with same space group, which is orbital dependent (Figs. S6-S7, S9-S14, S22-S23 [36]). Our theory also indicates there are two types of ZSPLs, one is unpinned (band-index dependent) and another is pinned (band-index independent). Finally, we predict the symmetry-constrained 3D PSTs can widely exist in two families of nonsymmorphic materials, which paves the way for designing the long-lifetime spintronic devices.

This work is supported by NSFC (Grants Nos. 12088101 and 12004030), the National Key Research and Development of China (Grant No. 2022YFA1402401), NSAF (Grant No. U2230402) and the Fundamental Research Funds for the Central Universities. Calculations were done in Tianhe-JK cluster at CSRC.

* These authors contributed equally to this work

† Email: bing.huang@csrc.ac.cn

- [1] X. Zhang, Q. Liu, J.-W. Luo, A. J. Freeman, and A. Zunger, *Nature Physics* **10**, 387 (2014).
 [2] L. Yuan, Q. Liu, X. Zhang, J.-W. Luo, S.-S. Li, and A. Zunger, *Nature Communications* **10**, 906 (2019).
 [3] L.-D. Yuan, X. Zhang, C. M. Acosta, and A. Zunger, *Nature*

Communications **14**, 5301 (2023).

- [4] S. Guan, J.-W. Luo, S.-S. Li, and A. Zunger, *Physical Review B* **107**, L081201 (2023).
 [5] A. Manchon, H. C. Koo, J. Nitta, S. M. Frolov, and R. A. Duine, *Nature Materials* **14**, 871 (2015).
 [6] V. M. Edelstein, *Solid State Communications* **73**, 233 (1990).
 [7] J. C. R. Sanchez, L. Vila, G. Desfonds, S. Gambarelli, J. P. Attan, J. M. De Teresa, C. Magn, and A. Fert, *Nature Communications* **4**, 2944 (2013).
 [8] K. Shen, G. Vignale, and R. Raimondi, *Physical Review Letters* **112**, 096601 (2014).
 [9] F. Calavalle, M. Surez-Rodriguez, B. Martn-Garca, A. Johansson, D. C. Vaz, H. Yang, I. V. Maznichenko, S. Osttanin, A. Mateo-Alonso, A. Chuvilin, I. Mertig, M. Gobbi, F. Casanova, and L. E. Hueso, *Nature Materials* **21**, 526 (2022).
 [10] L. Cai, C. Yu, W. Zhao, Y. Li, H. Feng, H.-A. Zhou, L. Wang, X. Zhang, Y. Zhang, Y. Shi, J. Zhang, L. Yang, and W. Jiang, *Nano Letters* **22**, 7441 (2022).
 [11] B. A. Bernevig and O. Vafeek, *Physical Review B* **72**, 033203 (2005).
 [12] A. Chernyshov, M. Overby, X. Liu, J. K. Furdyna, Y. Lyanda-Geller, and L. P. Rokhinson, *Nature Physics* **5**, 656 (2009).
 [13] A. Manchon, J. Ålezno, I. Miron, T. Jungwirth, J. Sinova, A. Thiaville, K. Garello, and P. Gambardella, *Reviews of Modern Physics* **91**, 035004 (2019).
 [14] E. Grimaldi, V. Krizakova, G. Sala, F. Yasin, S. Couet, G. Sankar Kar, K. Garello, and P. Gambardella, *Nature Nanotechnology* **15**, 111 (2020).
 [15] S. D. Ganichev, E. L. Ivchenko, V. V. Bel'kov, S. A. Tarasenko, M. Sollinger, D. Weiss, W. Wegscheider, and W. Prettl, *Nature* **417**, 153 (2002).
 [16] L. A. Bentez, W. Saverio Torres, J. F. Sierra, M. Timmermans, J. H. Garcia, S. Roche, M. V. Costache, and S. O. Valenzuela, *Nature Materials* **19**, 170 (2020).
 [17] D. Khokhriakov, A. M. Hoque, B. Karpiak, and S. P. Dash, *Nature Communications* **11**, 3657 (2020).
 [18] J. Fabian and S. D. Sarma, *Journal of Vacuum Science & Technology B: Microelectronics and Nanometer Structures Processing, Measurement, and Phenomena* **17**, 1708 (1999).
 [19] N. S. Averkiev and L. E. Golub, *Physical Review B* **60**, 15582 (1999).
 [20] J. D. Koralek, C. P. Weber, J. Orenstein, B. A. Bernevig, S.-C. Zhang, S. Mack, and D. D. Awschalom, *Nature* **458**, 610 (2009).
 [21] A. Balocchi, Q. H. Duong, P. Renucci, B. L. Liu, C. Fontaine, T. Amand, D. Lagarde, and X. Marie, *Physical Review Letters* **107**, 136604 (2011).
 [22] J. Schliemann, *Reviews of Modern Physics* **89**, 011001 (2017).
 [23] L. L. Tao and E. Y. Tsymlal, *Nature Communications* **9**, 2763 (2018).
 [24] K. Ishizaka, M. S. Bahramy, H. Murakawa, M. Sakano, T. Shimojima, T. Sonobe, K. Koizumi, S. Shin, H. Miyahara, A. Kimura, K. Miyamoto, T. Okuda, H. Namatame, M. Taniguchi, R. Arita, N. Nagaosa, K. Kobayashi, Y. Murakami, R. Kumai, Y. Kaneko, Y. Onose, and Y. Tokura, *Nature Materials* **10**, 521 (2011).
 [25] D. Di Sante, P. Barone, R. Bertacco, and S. Picozzi, *Advanced Materials* **25**, 509 (2013).
 [26] G. Dresselhaus, *Physical Review* **100**, 580 (1955).
 [27] M. Hirayama, R. Okugawa, S. Ishibashi, S. Murakami, and T. Miyake, *Physical Review Letters* **114**, 206401 (2015).
 [28] M. Sakano, M. Hirayama, T. Takahashi, S. Akebi, M. Nakayama, K. Kuroda, K. Taguchi, T. Yoshikawa, K. Miyamoto, T. Okuda, K. Ono, H. Kumigashira, T. Ideue,

- Y. Iwasa, N. Mitsuishi, K. Ishizaka, S. Shin, T. Miyake, S. Murakami, T. Sasagawa, and T. Kondo, *Physical Review Letters* **124**, 136404 (2020).
- [29] G. Gatti, D. Gosálbez-Martinez, S. Tsirkin, M. Fanciulli, M. Puppini, S. Polishchuk, S. Moser, L. Testa, E. Martino, S. Roth, P. Bugnon, L. Moreschini, A. Bostwick, C. Jozwiak, E. Rotenberg, G. Di Santo, L. Petaccia, I. Vobornik, J. Fujii, J. Wong, D. Jariwala, H. Atwater, H. Rnnow, M. Chergui, O. Yazyev, M. Grioni, and A. Crepaldi, *Physical Review Letters* **125**, 216402 (2020).
- [30] H. J. Zhao, H. Nakamura, R. Arras, C. Paillard, P. Chen, J. Gosteau, X. Li, Y. Yang, and L. Bellaiche, *Physical Review Letters* **125**, 216405 (2020).
- [31] C. Mera Acosta, L. Yuan, G. M. Dalpian, and A. Zunger, *Physical Review B* **104**, 104408 (2021).
- [32] M. Lin, I. Robredo, N. B. M. Schrter, C. Felser, M. G. Vergniory, and B. Bradlyn, *Physical Review B* **106**, 245101 (2022).
- [33] W. Tan, X. Jiang, Y. Li, X. Wu, J. Wang, and B. Huang, *Advanced Functional Materials* **32**, 2208023 (2022).
- [34] Y. Liu, J. Li, P. Liu, and Q. Liu, *arXiv e-prints*, arXiv:2306.16312 (2023).
- [35] D. Gosálbez-Martínez, A. Crepaldi, and O. V. Yazyev, *Phys. Rev. B* **108**, L201114 (2023).
- [36] See Supplemental Material for details about the computational methods, classification of all crystalline symmetry operations, crystal structures, Brillouin zones, band dispersions, spin textures, and 3D persistent spin textures for different systems, which also includes Refs. [43-45,50-53] .
- [37] Z. Lin, C. Wang, Y. Xu, and W. Duan, *Physical Review B* **102**, 165143 (2020).
- [38] J. Ji, F. Lou, R. Yu, J. S. Feng, and H. J. Xiang, *Physical Review B* **105**, L041404 (2022).
- [39] K. Liu, W. Luo, J. Ji, P. Barone, S. Picozzi, and H. J. Xiang, *Nature Communications* **10**, 5144 (2019).
- [40] S.-D. Guo, X.-K. Feng, D. Huang, S. Chen, G. Wang, and Y. S. Ang, *Physical Review B* **108**, 075421 (2023).
- [41] J. Wang, Y. Liu, K.-H. Jin, X. Sui, L. Zhang, W. Duan, F. Liu, and B. Huang, *Physical Review B* **98**, 201112 (2018).
- [42] G. Chang, B. J. Wieder, F. Schindler, D. S. Sanchez, I. Belopolski, S.-M. Huang, B. Singh, D. Wu, T.-R. Chang, T. Neupert, S.-Y. Xu, H. Lin, and M. Z. Hasan, *Nature Materials* **17**, 978 (2018).
- [43] B. Bradlyn, L. Elcoro, J. Cano, M. G. Vergniory, Z. Wang, C. Felser, M. I. Aroyo, and B. A. Bernevig, *Nature* **547**, 298 (2017).
- [44] M. G. Vergniory, L. Elcoro, C. Felser, N. Regnault, B. A. Bernevig, and Z. Wang, *Nature* **566**, 480 (2019).
- [45] M. G. Vergniory, B. J. Wieder, L. Elcoro, S. S. P. Parkin, C. Felser, B. A. Bernevig, and N. Regnault, *Science* **376**, abg9094 (2022).
- [46] B.-J. Yang, T. A. Bojesen, T. Morimoto, and A. Furusaki, *Physical Review B* **95**, 075135 (2017).
- [47] Bradlyn Barry, Cano Jennifer, Wang Zhijun, Vergniory M. G., Felser C., Cava R. J., and Bernevig B. Andrei, *Science* **353**, aaf5037 (2016).
- [48] B. Ghler, V. Hamelbeck, T. Z. Markus, M. Kettner, G. F. Hanne, Z. Vager, R. Naaman, and H. Zacharias, *Science* **331**, 894 (2011).
- [49] R. Nakajima, D. Hirobe, G. Kawaguchi, Y. Nabei, T. Sato, T. Narushima, H. Okamoto, and H. M. Yamamoto, *Nature* **613**, 479 (2023).
- [50] G. Kresse and J. Furthmller, *Computational Materials Science* **6**, 15 (1996).
- [51] G. Kresse and J. Furthmller, *Physical Review B* **54**, 11169 (1996).
- [52] J. P. Perdew, K. Burke, and M. Ernzerhof, *Physical Review Letters* **77**, 3865 (1996).
- [53] M. I. Aroyo, J. M. Perez-Mato, C. Capillas, E. Kroumova, S. Ivantchev, G. Madariaga, A. Kirov, and H. Wondratschek, *Zeitschrift für Kristallographie - Crystalline Materials* **221**, 15 (2006).